

# Three-Qubit-Embedded Split Cayley Hexagon is Contextuality Sensitive

Frédéric Holweck<sup>1,2</sup>, Henri de Boutray<sup>3</sup> and Metod Saniga<sup>4</sup>

<sup>1</sup>Laboratoire Interdisciplinaire Carnot de Bourgogne, ICB/UTBM, UMR 6303 CNRS, Université de Bourgogne Franche-Comté, 90010 Belfort Cedex, France

<sup>2</sup>Department of Mathematics and Statistics, Auburn University, Auburn, AL, USA

<sup>3</sup>ColibriTD, La Défense, Paris, France

<sup>4</sup>Astronomical Institute, Slovak Academy of Sciences, SK-05960 Tatranská Lomnica, Slovak Republic

(29 January 2022)

---

**Abstract:** It is known that there are two non-equivalent embeddings of the split Cayley hexagon of order two into  $\mathcal{W}(5, 2)$ , the binary symplectic polar space of rank three, called classical and skew. Labelling the 63 points of  $\mathcal{W}(5, 2)$  by the 63 canonical observables of the three-qubit Pauli group subject to the symplectic polarity induced by the (commutation relations between the elements of the) group, the two types of embedding are found to be quantum contextuality sensitive. In particular, we show that the complement of a classically-embedded hexagon is not contextual, whereas that of a skewly-embedded one is.

**Keywords:** finite geometry, quantum contextuality, Pauli groups, generalized polygons, Kochen-Specker Theorem, split Cayley hexagon of order two

---

## 1 Introduction

Quantum contextuality is one of the most counter-intuitive notions in quantum physics that is assumed to be of main importance in quantum information [1, 2, 3, 4]. Roughly speaking, quantum contextuality rules out any Hidden Variables Theory unless one assumes that the pre-existing values of a measurement depend on the context, i.e. on the set of mutually commuting measurements in which a given experience takes place. First proved mathematically by Kochen and Specker [5], several alternative proofs [6, 7] and experimental validations [8, 9] have been provided since then. For a recent comprehensive survey about contextuality, see [10].

Among various formulations of quantum contextuality we will deal in this paper with observable-based proofs of quantum contextuality as proposed by Mermin [11] and Peres [12]. In this formulation, see Section 2, a proof of the Kochen-Specker (KS) Theorem is provided by a configuration of sets of mutually commuting observables, called contexts, such that all the constraints imposed by the configuration on the eigenvalues of those observables cannot be satisfied by a classical function unless that function is context-dependent. We will call such a configuration *contextual* when it furnishes a proof of the KS Theorem. These proofs of contextuality can also be tested experimentally [13, 14, 15]. Interestingly, this type of contextual configurations, which involves  $N$ -qubit Pauli observables, can be embedded as subgeometries of the geometric realization of the  $N$ -qubit Pauli group known as the symplectic polar space of rank  $N$  and order two, usually denoted as  $\mathcal{W}(2N - 1, 2)$ , see Section 2. This geometric perspective on  $N$ -qubit observables was introduced some 15 years ago [16, 17, 18] and led to several surprising connections between physics and geometry [19] and also between different branches of modern physics, like, for instance, the so-called black-hole/qubit correspondence [20, 21].

In  $\mathcal{W}(5, 2)$  one can find a number of copies of a very special configuration made of 63 points and 63 lines, called the split Cayley hexagon of order two. This configuration is a generalized hexagon in the sense that it is  $m$ -gon free for  $m \leq 5$ . The fact that it can be embedded into the three-qubit polar space,  $\mathcal{W}(5, 2)$ , was first employed in [22] to establish

connections between three-qubit observables and black-hole entropy formulas. Later it was also proved that this configuration has, in fact, two distinguished embeddings in  $\mathcal{W}(5, 2)$ , one called classical, the other skew [23]. In this article one shows that these two distinguished embeddings behave differently in terms of contextuality. More precisely, if one denotes the two embeddings by  $\mathcal{H}_C$  and  $\mathcal{H}_S$ , respectively, then one demonstrates that the configuration  $\overline{\mathcal{H}}_C = \mathcal{W}(5, 2) \setminus \mathcal{H}_C$ , i.e. the configuration made of all the line-contexts that are in  $\mathcal{W}(5, 2)$  but not in  $\mathcal{H}_C$ , is not contextual, while  $\overline{\mathcal{H}}_S = \mathcal{W}(5, 2) \setminus \mathcal{H}_S$  is contextual.

The paper is organized as follows. In Section 2 we recall the basic notions on observable-based proofs of contextuality as well as the notion of symplectic polar spaces where corresponding configurations live. We also explain how we prove that a given configuration is contextual by solving a particular linear system. In Section 3 one details the differences between the two distinguished symplectic embeddings of the split Cayley hexagon of order two and recall some known results about these specific configurations. Finally in Section 4 we collect our results and state precisely our hexagon-related contextuality findings. Section 5 concludes this paper with general remarks and perspectives.

## 2 Observable-based proofs of contextuality and the symplectic polar spaces over the two-element field

Let us recall the principle of the Mermin and Peres [11, 12] operator-based proofs of quantum contextuality. Consider the configuration of two-qubit observables depicted in Figure 1 and known as a Peres-Mermin magic square.

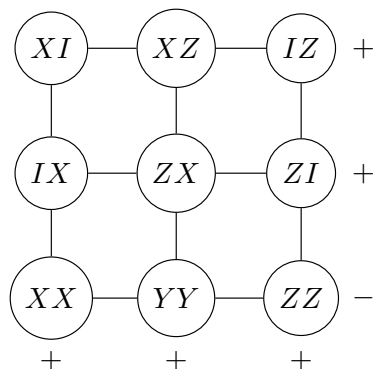


Figure 1: The Peres-Mermin magic square: All two-qubit observables on the same row/column mutually commute. The product of observables in each row/column is equal to  $\pm I_4$  as indicated by the signs. The measurement of each two-qubit observable yields  $\pm 1$ . One observes that there is no deterministic classical function that would predict the outcomes for each node and satisfy all the signs constraints.

Each node of the square is labelled by a two-qubit observable with a shorthanded notation  $AB \equiv A \otimes B$ . Here  $A, B \in \{I, X, Y, Z\}$  with  $X, Y, Z$  being the usual Pauli matrices and  $I$  the unit matrix. In each row/column of the grid, two-qubit observables mutually commute and form what we call a context, i. e. a set of compatible measurements whose product is, up to a sign, the identity operator. In the Peres-Mermin square the product of the observables on each context is  $\pm I_4$  as indicated by the signs in Figure 1. In each context, the product of the measurements, which are eigenvalues of the observables, should be an eigenvalue of the product of the observables. The eigenvalues of each node are  $\pm 1$  and the constraint on each context is  $\pm 1$  according to the signs prescription on rows/columns. Because there is an odd number of negative contexts in the square, it is clear that there exists no classical function that can assign predefined values to each node and satisfy all the constraints imposed by the signs of the contexts (rows/columns). If such a classical function existed, it would necessarily be context-dependent, i. e. the predefined value assigned to a given node would depend on

the considered context. This elementary configuration of observables furnishes a proof of the KS Theorem by showing that there is no Non-Contextual Hidden Variable (NCHV) theory that can reproduce the outcomes of quantum physics. Another elementary proof based on three-qubit observables was proposed by Mermin in [11] and is reproduced in Figure 2.

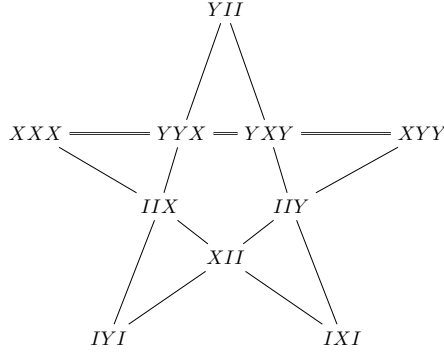


Figure 2: The Mermin pentagram [11]. Each node is labelled by a three-qubit Pauli observable. The lines of the pentagram are sets of mutually commuting observables whose product is  $+I_8$  (each thin line) or  $-I_8$  (the double line). The fact that there is only one (odd number) negative line allows us to use the same argument as for the Peres-Mermin magic square. This configuration therefore also furnishes a proof of the KS Theorem.

In [24] it was proved that Peres-Mermin magic squares and Mermin pentagrams are the smallest possible proofs of the KS Theorem that can be achieved in terms of the number of observables and contexts: 9 observables and 6 contexts for the Peres-Mermin magic square and 10 observables and 5 contexts for the pentagram.

If one considers two-qubit Pauli observables up to a global phase  $(\pm 1, \pm i)$ , there are 10 copies of the magic square. One explains now how one can naturally embed these 10 grids into the symplectic polar space of rank  $N = 2$  over the two-elements field  $\mathbb{F}_2 = \{0, 1\}$ . In full generality let us consider the group of  $N$ -qubit Pauli observables, i.e.

$$\mathcal{P}_N = \{sA_1A_2 \dots A_N, s \in \{\pm 1, \pm i\}, A_i \in \{I, X, Y, Z\}\}, \quad (1)$$

employing again the shorthand notation  $A_1A_2 \dots A_N \equiv A_1 \otimes A_2 \otimes \dots \otimes A_N$ . The center of  $\mathcal{P}_N$  is  $\mathcal{C}_N = \{\pm I_{2^N}, \pm iI_{2^N}\}$ . The abelian group  $\mathcal{P}_N/\mathcal{C}_N$  is isomorphic to the  $2N$ -dimensional vector space  $V_N = \mathbb{F}_2^{2N}$  as we now explain.

Up to a phase, each observable  $A_i$  can be represented by a doublet  $(\mu_i, \nu_i) \in \mathbb{F}_2^2$  as follows

$$A_i = Z^{\mu_i} \cdot X^{\nu_i} \text{ where } \cdot \text{ denotes the ordinary product of matrices;} \quad (2)$$

more precisely, we have the following relations:

$$I \leftrightarrow (0, 0), X \leftrightarrow (0, 1), Z \leftrightarrow (1, 0), iY \leftrightarrow (1, 1). \quad (3)$$

Hence, to a given class  $\bar{\mathcal{O}} = \{A_1A_2 \dots A_N, -A_1A_2 \dots A_N, iA_1A_2 \dots A_N, -iA_1A_2 \dots A_N\}$  in  $\mathcal{P}_N/\mathcal{C}_N$  one can associate a unique  $2N$ -plet  $(\mu_1, \nu_1, \dots, \mu_N, \nu_N) \in \mathbb{F}_2^{2N}$ . Moreover, the multiplicative structure of  $\mathcal{P}_N/\mathcal{C}_N$  is mapped to the additive structure of  $V_N$ . Considering now the projective space associated with  $V_N$ ,  $PG(2N - 1, 2)$ , one obtains a map between non-trivial  $N$ -qubit observables, up to a global phase, and points of  $PG(2N - 1, 2)$

$$\pi : \begin{cases} (\mathcal{P}_N/\mathcal{C}_N) \setminus I_{2^N} & \rightarrow PG(2N - 1, 2), \\ \mathcal{O} & \mapsto [\mu_1 : \nu_1 : \mu_2 : \nu_2 : \dots : \mu_N : \nu_N]. \end{cases} \quad (4)$$

This mapping represents (classes of) observables as points in  $PG(2N - 1, 2)$ , but tells us nothing about the commutation relations in  $\mathcal{P}_N$ . In order to recover this information, one

introduces the following symplectic form on  $PG(2N - 1, 2)$ :

$$\langle p, q \rangle = \sum_{i=1}^N p_i q_{N+i} + p_{N+i} q_i, \quad (5)$$

where  $p = [p_1 : \dots : p_{2N}]$  and  $q = [q_1 : \dots : q_{2N}] \in PG(2N - 1, 2)$ . Then, if one considers two non-trivial classes  $\overline{\mathcal{O}}_p$  and  $\overline{\mathcal{O}}_q$  of  $N$ -qubit Pauli observables in  $\mathcal{P}_N/\mathcal{C}_N$  such that  $\pi(\overline{\mathcal{O}}_p) = p$  and  $\pi(\overline{\mathcal{O}}_q) = q$ , then a straightforward calculation shows that

$$\overline{\mathcal{O}}_p \text{ and } \overline{\mathcal{O}}_q \text{ commute} \Leftrightarrow \langle p, q \rangle = 0. \quad (6)$$

Employing the above-defined symplectic form leads to the definition of  $\mathcal{W}(2N - 1, 2)$ , the symplectic polar space of rank  $N$  and order 2.

**Definition 1.** The space of totally isotropic subspaces<sup>1</sup> of  $PG(2N - 1, 2)$  endowed with a nondegenerate symplectic form  $\langle, \rangle$  is called the symplectic polar space of rank  $N$  and order 2,  $\mathcal{W}(2N - 1, 2)$ .

Note that because of the symplectic form, the group  $\text{Sp}(2N, 2)$  of symplectic matrices acts transitively on  $\mathcal{W}(2N - 1, 2)$ . This group is spanned by the transvections  $T_p$  for all  $p \in \mathcal{W}(2N - 1, 2)$ :

$$T_p : \begin{cases} \mathcal{W}(2N - 1, 2) & \rightarrow & \mathcal{W}(2N - 1, 2), \\ q & \mapsto & q + \langle p, q \rangle p. \end{cases} \quad (7)$$

If we consider the action of transvections in terms of the labelling of  $\mathcal{W}(2N - 1, 2)$  by  $N$ -qubit Pauli observables, then for  $p = \pi(\overline{\mathcal{O}}_p)$  and  $q = \pi(\overline{\mathcal{O}}_q)$  we have

$$T_{\overline{\mathcal{O}}_p}(\overline{\mathcal{O}}_q) = \begin{cases} \overline{\mathcal{O}}_q & \text{if and only if } \overline{\mathcal{O}}_p \text{ and } \overline{\mathcal{O}}_q \text{ commute,} \\ \overline{\mathcal{O}}_q \cdot \overline{\mathcal{O}}_p & \text{if and only if } \overline{\mathcal{O}}_p \text{ and } \overline{\mathcal{O}}_q \text{ anticommute.} \end{cases} \quad (8)$$

The points of  $\mathcal{W}(2N - 1, 2)$  are  $N$ -qubit observables, lines correspond to triplet of mutually commuting elements whose product is  $\pm I_N$  and form contexts. Planes and higher dimensional linear subspaces of  $\mathcal{W}(2N - 1, 2)$  can also be of some use to generate contexts. Let us illustrate this for  $N = 2$  and  $N = 3$  [25, 26].

## 2.1 $N = 2$ , the Doily $\mathcal{W}(3, 2)$

The symplectic polar space of rank 2 and order 2, known as the doily, encapsulates the commutation relations within the two-qubit Pauli group. This space features 15 points and 15 lines and form a  $15_3$  configuration, i.e. a point-line incidence structure with 3 points per line and 3 lines per point. Out of 245,342 non isomorphic  $15_3$ -configurations, the doily is the only one to be *triangle free*. Using the canonical representatives ( $s = 1$  in (1)), one gets a labelling of the doily by two-qubit Pauli observables as given in Figure 3.

Peres-Mermin magic squares are subgeometries of  $\mathcal{W}(3, 2)$ . More precisely they are geometric hyperplanes of  $\mathcal{W}(3, 2)$ , i.e. sets of points such that a line of  $\mathcal{W}(3, 2)$  is either fully contained in such set or shares with it a single point. An example of such a set is given in Figure 4. Starting with this canonical labeling one can form 9 more copies of Peres-Mermin square by acting by transvections. Each of them have an odd number, namely 1 or 3, of negative contexts and is thus contextual.

To conclude this subsection it is worth mentioning that the space  $\mathcal{W}(3, 2)$  of its own is a contextual configuration, as first proved in [13]. In fact, Cabello shows that the configuration corresponding to points and lines of  $\mathcal{W}(2N - 1, 2)$  is contextual for any  $N \geq 2$ .

<sup>1</sup>A linear space is said to be totally isotropic if and only if the symplectic form vanishes identically on the space.

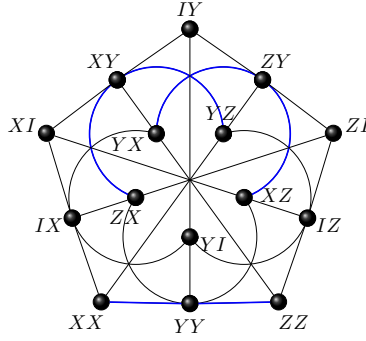


Figure 3: The symplectic polar space  $\mathcal{W}(3, 2)$  labelled by two-qubit Pauli observables. Each line of the configuration forms a context. The three negative contexts are indicated in blue.

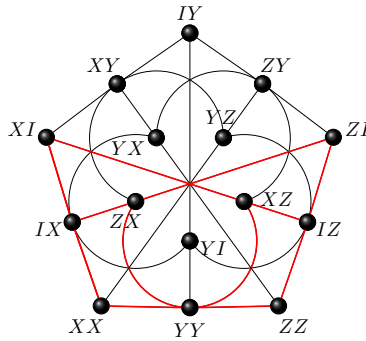


Figure 4: A Peres-Mermin square as a subgeometry of the doily. The square is the same as the one introduced in Figure 1. It is a geometric hyperplane in the sense that a line of  $\mathcal{W}(3, 2)$  is either contained in it (six such lines depicted in red) or has one point common with it (each of the remaining nine lines).

## 2.2 $N = 3$ , the symplectic polar space $\mathcal{W}(5, 2)$

The symplectic polar space of rank 3,  $\mathcal{W}(5, 2)$ , comprises 63 points, 315 lines and 135 Fano planes. An interesting study of geometric hyperplanes of  $\mathcal{W}(5, 2)$  and their physical interpretations in terms of representation theory and invariants can be found in [26]. Fano planes of  $\mathcal{W}(5, 2)$  are totally isotropic 2-dimensional spaces over  $\mathbb{F}_2$ . An example of such a plane is given in Figure 5. The product of the seven observables in a Fano plane yields  $\pm I_8$ . If one removes a line, one gets a new type of context – an affine plane of order two – made of four observables whose product is  $\pm I_8$ . For instance, in the negative Fano plane of Figure 5, removing the line  $ZZI - IZZ - ZIZ$ , which is positive, leads to the context  $XXX - YYX - YXY - XYY$  that is exactly the negative line of the Mermin pentagram of Figure 2. Using three-qubit Pauli operator contexts of this type one can create altogether 12,096 distinct Mermin’s pentagrams in  $\mathcal{W}(5, 2)$ , as it was first shown by computer calculations [27] and later proved also rigorously by sole geometric arguments [28]. In [29] it was demonstrated that geometric hyperplanes of  $\mathcal{W}(5, 2)$  defined by quadratic equations (hyperbolic or elliptic) are also contextual configurations; contextual inequalities for the hyperbolic case were also tested on a quantum computer [15].

In Section 3 we will introduce another prominent configuration, namely the split Cayley hexagon of order two, which lives in  $\mathcal{W}(5, 2)$  in two distinct modes featuring *different* contextuality behavior.

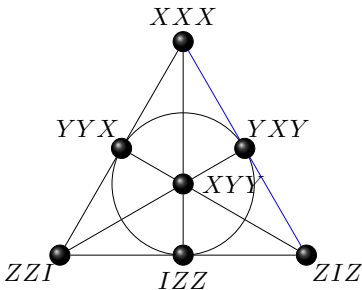


Figure 5: An example of the (negative) Fano plane in  $\mathcal{W}(5, 2)$ ; the blue line is also negative.

### 2.3 A simple method for checking contextuality of a configuration

In order to prove that a particular point-line configuration of observables, i.e. a set of observables  $\{\mathcal{O}_j\}_{j \in J}$  grouped into contexts  $\{\mathcal{C}_i\}_{i \in I}$ , provides a KS proof, we reformulate the question as a linear problem [29]. Indeed, the existence of an NCHV theory that accommodates all contexts  $\mathcal{C}_i$  of a configuration means that there exists a classical function,  $f$ , such that  $f(\mathcal{O}_j) = \pm 1$  for all observables and for all contexts  $\mathcal{C}_i$  of the configuration. This means that  $f$  satisfies the following system of equations:

$$\prod_{\mathcal{O}_j \in \mathcal{C}_i} f(\mathcal{O}_j) = \text{sign}(\mathcal{C}_i), \forall i \in I, \quad (9)$$

where  $\text{sign}(\mathcal{C}_i)$  is the sign of the context  $\mathcal{C}_i$ .

Consider now the incidence matrix  $A$  of the configuration, i.e. an  $I \times J$  matrix where  $a_{ij} = 1$  if and only if  $\mathcal{O}_j \in \mathcal{C}_i$  and  $a_{ij} = 0$  otherwise. Let  $b \in \mathbb{F}_2^I$  such that  $b_i = 0$  if and only if  $\text{sign}(\mathcal{C}_i) = 1$  and  $b_i = 1$  if and only if  $\text{sign}(\mathcal{C}_i) = -1$ . Then the existence of a classical function  $f$  that satisfies the constraints of Eq. (9) boils down to finding a vector  $x \in \mathbb{F}_2^J$  which is the solution of the following linear system

$$Ax = b. \quad (10)$$

For instance, in the case of the Peres-Mermin configuration of Figure 1 the linear system to be solved over the two-element field is

$$\begin{pmatrix} 1 & 1 & 1 & 0 & 0 & 0 & 0 & 0 & 0 \\ 0 & 0 & 0 & 1 & 1 & 1 & 0 & 0 & 0 \\ 0 & 0 & 0 & 0 & 0 & 0 & 1 & 1 & 1 \\ 1 & 0 & 0 & 1 & 0 & 0 & 1 & 0 & 0 \\ 0 & 1 & 0 & 0 & 1 & 0 & 0 & 1 & 0 \\ 0 & 0 & 1 & 0 & 0 & 1 & 0 & 0 & 1 \end{pmatrix} \cdot \begin{pmatrix} x_1 \\ x_2 \\ x_3 \\ x_4 \\ x_5 \\ x_6 \\ x_7 \\ x_8 \\ x_9 \end{pmatrix} = \begin{pmatrix} 0 \\ 0 \\ 0 \\ 0 \\ 0 \\ 0 \\ 0 \\ 0 \\ 1 \end{pmatrix}. \quad (11)$$

One readily sees that this system has no solution as the sum of the first five rows of  $A$  equals the last row, while the sum of the first five coordinates of  $b$  does not equal the last coordinate. The lack of solution means that the corresponding configuration is contextual, i.e. it furnishes a proof of the KS Theorem. This linear formulation of the problem allows us to get a relatively fast computer-based check of the contextual nature of larger sets of contexts and observables. Note that the incidence matrix  $A$  encodes the geometry of the configuration, while the vector  $b$  encodes the signs of the contexts; the latter, of course, depends on the choice of labeling of the points of the symplectic polar space by  $N$ -qubit observables.

### 3 The split Cayley hexagon of order two and its two non-equivalent symplectic embeddings

A generalized  $n$ -gon  $\mathcal{G}$  of order  $(k, l)$  is an point-line incidence structure such that every line contains  $k + 1$  points, every point is contained in  $l + 1$  lines and  $\mathcal{G}$  does not contain any ordinary  $m$ -gons for  $2 \leq m < n$ , but two points, two lines or a point and a line are always contained in an  $n$ -gon [30]. When  $k = l$  one says that the order of  $\mathcal{G}$  is  $k$ . The Fano plane, Figure 5, is the unique example of the generalized triangle of order two and the doily  $\mathcal{W}(3, 2)$ , Figure 3, is the unique (self-dual) generalized quadrangle of order two. There is no generalized 5-gon of order two, but there exist two generalized hexagons of order two, the split Cayley hexagon and its dual [30]. We will focus now on the split Cayley hexagon,  $\mathcal{H}$ , which also lives in  $\mathcal{W}(5, 2)$ ; this means that one can label the 63 points of  $\mathcal{H}$  by the 63 non trivial three-qubit observables in such a way that the lines of the hexagon are lines of  $\mathcal{W}(5, 2)$ , i. e. sets of mutually commuting three-qubit observables.

As already stressed, there are two unequivalent embeddings of  $\mathcal{H}$  in  $\mathcal{W}(5, 2)$ . The first one, called classical, was explicitly worked out in [22] and in the context of quantum information further discussed, for instance, in [20, 27, 32]; an example of such embedding is portrayed in Figure 6.

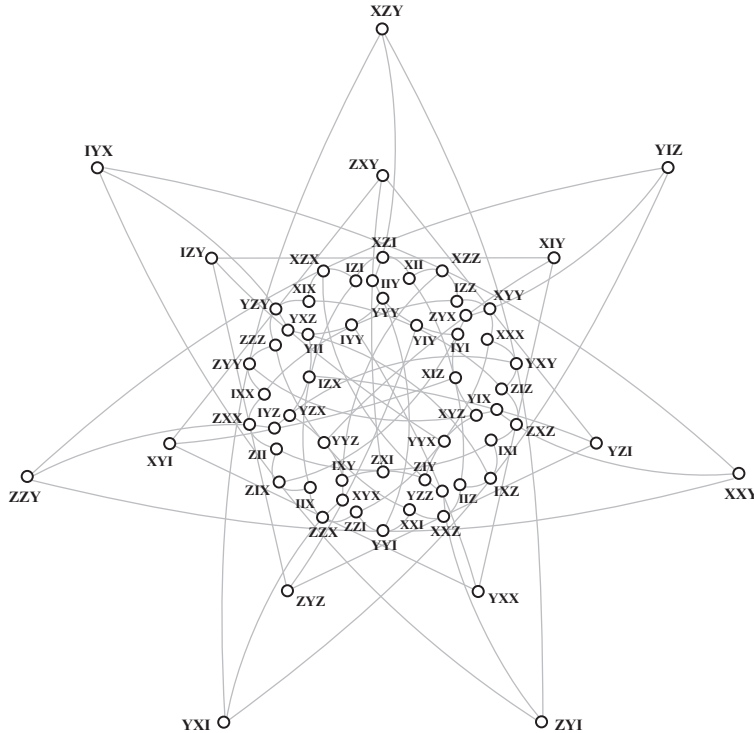


Figure 6: Three-qubit *classical* embedding of the split Cayley hexagon of order two as described in [22]. The illustration of points and lines of the hexagon follows closely that of Ref. [31]

In  $\mathcal{W}(5, 2)$  there are 120 classically-embedded copies of  $\mathcal{H}$ ; each of them can be obtained from the copy shown in Figure 6 by the action of the symplectic group  $\text{Sp}(6, 2)$ . The labelling of Figure 6 was obtained from the observation that the split Cayley hexagon contains a copy of the Heawood graph, the incidence graph of the Fano plane, and following the procedure outlined in [33].

Another description of this embedding is the following one [30]. In  $\text{PG}(6, 2)$ , consider

the following parabolic quadric  $\mathcal{Q}$

$$x_1x_4 + x_2x_5 + x_3x_6 - x_7^2 = 0. \quad (12)$$

This quadric contains 63 points. Consider now the lines of  $\mathcal{Q}$  that satisfy the following Plücker equations:

$$\begin{aligned} p_{62} = p_{17}, \quad p_{13} = p_{72}, \quad p_{24} = p_{37}, \quad p_{35} = p_{74}, \\ p_{46} = p_{57}, \quad p_{51} = p_{76}, \quad p_{14} + p_{25} + p_{36} = 0, \end{aligned} \quad (13)$$

where  $p_{ij} = x_ix_j - x_jx_i$ . There are 63 such lines and the obtained  $63_3$  configuration is isomorphic to  $\mathcal{H}$ . This configuration can be bijectively projected into  $PG(5, 2)$  and  $\mathcal{W}(5, 2)$ . Indeed the projection

$$[x_1 : \cdots : x_7] \mapsto [x_1 : \cdots : x_6] \quad (14)$$

is a bijection over  $\mathbb{F}_2$  as  $x_7 = x_1x_2 + x_3x_4 + x_5x_6$  and the lines of  $\mathcal{Q}$  that satisfy the Plücker relations (13) are mapped to totally isotropic lines of  $PG(5, 2)$ , i. e. the lines of  $\mathcal{W}(5, 2)$  for the symplectic form (5). This embedding will be denoted by  $\mathcal{H}_C$ .

Interestingly, there exists another, non-equivalent embedding of  $\mathcal{H}$  into  $\mathcal{W}(5, 2)$ , as discovered by Coolsaet [23]. Coolsaet considers, in  $PG(6, 2)$ , the following coordinate map

$$\epsilon : [x_1 : \cdots : x_7] \mapsto [x_1 + x_6 + f_5(x) : x_2 + x_3 + f_4(x) : x_3 : x_4 : x_5 : x_6 : x_7] \quad (15)$$

with  $f_4(x) = x_3x_5 + x_7x_4$  and  $f_5(x) = x_4x_6 + x_7x_5$ , which indeed establishes a different type of embedding of  $\mathcal{H}$  into  $\mathcal{Q}$ , called skew; its projection to  $\mathcal{W}(5, 2)$  will be denoted by  $\mathcal{H}_S$ . There are altogether 7560 copies of  $\mathcal{H}_S$  in  $\mathcal{W}(5, 2)$ ; one of them is depicted in Figure 7.

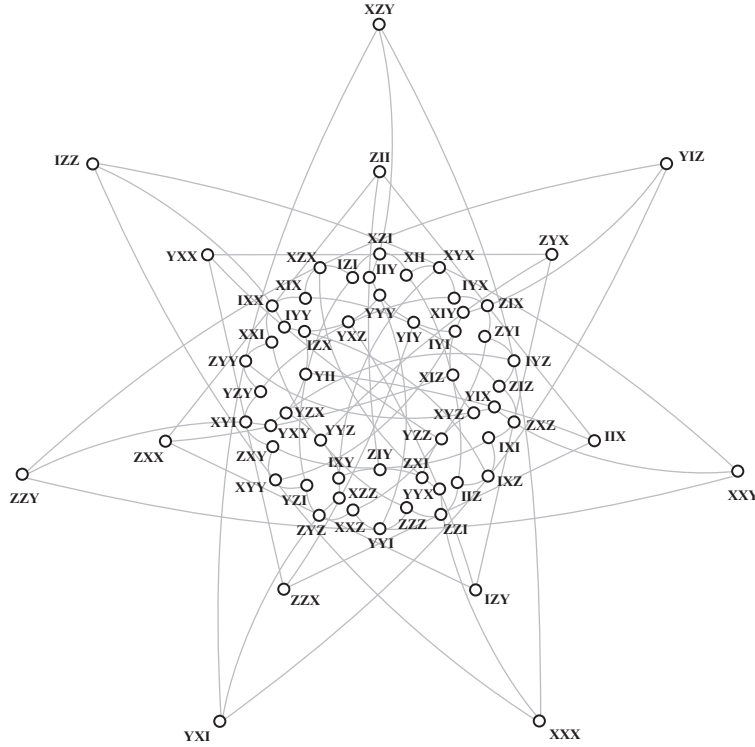


Figure 7: A copy of the split Cayley hexagon of order two that is skew-embedded into  $\mathcal{W}(5, 2)$ .



We shall conclude this section by a brief description of the main difference between the two embeddings. In  $\mathcal{H}_C$ , all the three lines passing through any of its points are coplanar, i. e. lie in the same plane of  $\mathcal{W}(5, 2)$ . This is, however, not the case for  $\mathcal{H}_S$ , where only 15 points exhibit this property; for each of the remaining 48 points, only two of the three lines are coplanar. To illustrate this, let us take the point  $XXX$  of the copy shown in Figure 7. The three lines passing through it are  $\{XXX, XYY, IZZ\}$ ,  $\{XXX, ZZI, YYX\}$  and  $\{XXX, IYZ, XZY\}$ ; clearly, only the first two lie in the same plane. Next, take any observable and all the 30 other observables that commute with it. These 31 observables will form a geometric hyperplane in both  $\mathcal{H}_C$  and  $\mathcal{H}_S$ . But the two embeddings differ in that while this hyperplane is of the same type for each point of  $\mathcal{H}_C$ , an  $\mathcal{H}_S$  features two different kinds of them.

## 4 $\overline{\mathcal{H}}_S$ is contextual, whereas $\overline{\mathcal{H}}_C$ is not!

At this point an interesting question arises: Can the two embeddings be ascribed some physical distinction? To answer this question (in affirmative), we ran several different experiments on  $\mathcal{W}(5, 2)$ ,  $\mathcal{H}'_C$ ,  $\mathcal{H}'_S$  and their complements. By the complement,  $\overline{\mathcal{G}}$ , of a configuration  $\mathcal{G} \subset \mathcal{W}(2N - 1, 2)$  we mean the set of all line-contexts of  $\mathcal{W}(2N - 1, 2)$  that are not in  $\mathcal{G}$ . We tested by computer the contextual nature of all  $\mathcal{H}_C, \mathcal{H}_S, \overline{\mathcal{H}}_C, \overline{\mathcal{H}}_S$  of  $\mathcal{W}(5, 2)$  and the results of our analysis are summarized in Table 1.

Geometry	Contextual	# of Copies
$\mathcal{H}_C$	No	120
$\mathcal{H}_S$	No	7560
$\overline{\mathcal{H}}_C$	No	120
$\overline{\mathcal{H}}_S$	Yes	7560

Table 1: Results on the contextuality properties of differently-embedded hexagons and their complements. The difference between the two embeddings reveals itself in terms of contextuality when one considers the complement of the configuration.

Our calculations were performed with the software Magma and the computation resources of the supercomputer of the Mésocentre de calcul de Franche-Comté. All our codes and results are available on the QuantCert GitHub page<sup>2</sup>. To implement the incidence structures of  $\mathcal{H}_C$  and  $\mathcal{H}_S$  we first encoded the description in coordinates of the two embeddings provided by Coolsaet [23] (Eq. (12), Eq. (13) and Eq. (15)). Then we created all 120 copies of  $\mathcal{H}_C$  and all 7560 copies of  $\mathcal{H}_S$  by repeatedly acting by transvections. Their complements were easily obtained from the implementation of  $\mathcal{W}(5, 2)$ . Once all incidence structures were created we checked their contextuality by using the function `IsConsistent` that establishes if a given configuration is contextual by employing the procedure described in Section 2.

The `IsConsistent` Magma intrinsic (compiled function) checks if the rank of the augmented matrix  $(A|b)$  is greater than the one of the coefficient matrix  $A$ . This operation is in  $O(|\mathcal{O}| + |\mathcal{C}|)$  operations; in other words, its execution lasts a time proportional to the number of observables and contexts of the geometry. Given the fact that this precise system had  $315 - 63 = 252$  contexts, the duration of this operation is quite negligible, even repeated several thousands of times. Building the 7560 copies of  $\mathcal{H}_S$  was more intensive though: to reach all copies we started with a single copy of  $\mathcal{H}_S$  and ran every possible combination of 4 transvections, including the identity, for a total of  $64^4 = 2^{24} \approx 17E6$  total operations. This computation lasted around 11 hours (10.87 to be more precise), which speaks for the efficiency of Magma.

<sup>2</sup>URL: <https://quantcert.github.io/Magma-contextuality/>

## 5 Conclusion

We have found a very important physical property regarding the two non-equivalent embeddings of a very special subconfiguration of the symplectic polar space  $\mathcal{W}(5, 2)$ , the split Cayley hexagon of order two. Using the interpretation in terms of three-qubit Pauli observables we showed that the complement of any skew-embedded hexagon is a contextual configuration, i.e. provides a proof of the Kochen-Specker Theorem. We tested our findings on all possible embeddings of the split Cayley hexagons and found out that only skew embeddings enjoy this property. To extend this work one may try to measure the degree of contextuality of  $\overline{\mathcal{H}}_S$ . The degree of contextuality indicates how far is a given contextual configuration to be satisfiable, i.e. non-contextual, if one changes the constraints imposed by the vector  $b$ . In other words, if  $|J|$  is the number of contexts and  $P$  the maximum number of constraints that can be satisfied, then the degree of contextuality is  $d = |J| - P$ . For a non-contextual configuration  $d = 0$ . The calculation of  $d$  boils down to finding the Hamming distance between  $b$  and the image of  $A$ , the incidence matrix of the configuration. However, in the case of the split Cayley hexagon a brute force calculation to compute  $d$  is out of reach of the supercomputer resources we have currently at our disposal. It, therefore, requires a deeper understanding of the geometry to reduce the calculation cost. The degree of contextuality  $d$  is also necessary for calculating the classical bound of the contextual inequalities given in [13] as well as for a possible testing of these inequalities on a quantum computer [15].

## 6 Acknowledgements

This work was supported by the Conseil Régional de Bourgogne Franche-Comté, mobility grant **GeoQuant**, the Thomas Jefferson Foundation and by the Slovak VEGA Grant Agency, Project # 2/0004/20. Part of this work was done during a visit of HdB and a one-year stay of FH at the Mathematics and Statistics Department of Auburn University. Both authors wish to acknowledge the people of the department that made our work here possible, in particular Dr. Luke Oeding for his precious help and friendship as well as Drs. Gaetan Bakalli and Mucyo Karemera for their hospitality and enthusiastic discussions about mathematics and life.

## References

- [1] Howard, M., Wallman, J., Veitch, V., & Emerson, J. (2014). Contextuality supplies the ‘magic’ for quantum computation. *Nature*, 510(7505), 351-355.
- [2] Bermejo-Vega, J., Delfosse, N., Browne, D. E., Okay, C., & Raussendorf, R. (2017). Contextuality as a resource for models of quantum computation with qubits. *Physical review letters*, 119(12), 120505.
- [3] Lillystone, P., Wallman, J. J., & Emerson, J. (2019). Contextuality and the single-qubit stabilizer subtheory. *Physical review letters*, 122(14), 140405.
- [4] Shahandeh, F. (2021). Quantum computational advantage implies contextuality. arXiv preprint [arXiv:2112.00024](https://arxiv.org/abs/2112.00024).
- [5] Kochen, S., & Specker, E. P. (1975). The problem of hidden variables in quantum mechanics. In *The logico-algebraic approach to quantum mechanics* (pp. 293-328). Springer, Dordrecht.
- [6] Lisoněk, P., Badziąg, P., Portillo, J. R., & Cabello, A. (2014). Kochen-Specker set with seven contexts. *Physical Review A*, 89(4), 042101.
- [7] Cabello, A., Kleinmann, M., & Portillo, J. R. (2016). Quantum state-independent contextuality requires 13 rays. *Journal of Physics A: Mathematical and Theoretical*, 49(38), 38LT01.

- [8] Bartosik, H., Klepp, J., Schmitzer, C., Sponar, S., Cabello, A., Rauch, H., & Hasegawa, Y. (2009). Experimental test of quantum contextuality in neutron interferometry. *Physical review letters*, 103(4), 040403.
- [9] D'Ambrosio, V., Herbauts, I., Amselem, E., Nagali, E., Bourennane, M., Sciarrino, F., & Cabello, A. (2013). Experimental implementation of a Kochen-Specker set of quantum tests. *Physical Review X*, 3(1), 011012.
- [10] Budroni, C., Cabello, A., Gühne, O., Kleinmann, M., & Larsson, J. Å. (2021). Quantum contextuality. arXiv preprint [arXiv:2102.13036](https://arxiv.org/abs/2102.13036).
- [11] Mermin, N. D. (1993). Hidden variables and the two theorems of John Bell. *Reviews of Modern Physics*, 65(3), 803.
- [12] Peres, A. (1990). Incompatible results of quantum measurements. *Physics Letters A*, 151(3-4), 107-108.
- [13] Cabello, A. (2010). Proposed test of macroscopic quantum contextuality. *Physical Review A*, 82(3), 032110.
- [14] Dikme, A., Reichel, N., Laghaout, A., & Björk, G. (2020). Measuring the Mermin-Peres magic square using an online quantum computer. arXiv preprint [arXiv:2009.10751](https://arxiv.org/abs/2009.10751).
- [15] Holweck, F. (2021). Testing quantum contextuality of binary symplectic polar spaces on a Noisy Intermediate Scale Quantum Computer. *Quantum Information Processing* 7/2021
- [16] Saniga, M., & Planat, M. (2007). Multiple Qubits as Symplectic Polar Spaces of Order Two. *Advanced Studies in Theoretical Physics*, 1, 1-4.
- [17] Thas, K. (2009). The geometry of generalized Pauli operators of N-qudit Hilbert space, and an application to MUBs. *EPL (Europhysics Letters)*, 86(6), 60005.
- [18] Havlicek, H., Odehnal, B., & Saniga, M. (2009). Factor-group-generated polar spaces and (multi-) qudits. *SIGMA. Symmetry, Integrability and Geometry: Methods and Applications*, 5, 096.
- [19] Saniga, M., Planat, M., & Rosu, H. (2004). Mutually unbiased bases and finite projective planes. *Journal of Optics B: Quantum and Semiclassical Optics*, 6(9), L19.
- [20] Lévay, P., Saniga, M., Vrana, P., & Pracna, P. (2009). Black hole entropy and finite geometry. *Physical Review D*, 79(8), 084036.
- [21] Lévay, P., & Holweck, F. (2019). Finite geometric toy model of spacetime as an error correcting code. *Physical Review D*, 99(8), 086015.
- [22] Lévay, P., Saniga, M., & Vrana, P. (2008). Three-qubit operators, the split Cayley hexagon of order two, and black holes. *Physical Review D*, 78(12), 124022.
- [23] Coolsaet, K. (2010). The smallest split Cayley hexagon has two symplectic embeddings. *Finite Fields and Their Applications*, 16(5), 380-384.
- [24] Holweck, F., & Saniga, M. (2017). Contextuality with a small number of observables. *International Journal of Quantum Information*, 15(04), 1750026.
- [25] Saniga, M., Planat, M., Pracna, P., & Havlicek, H. (2007). The Veldkamp space of two-qubits. *SIGMA. Symmetry, Integrability and Geometry: Methods and Applications*, 3, 075.
- [26] Lévay, P., Holweck, F., & Saniga, M. (2017). Magic three-qubit Veldkamp line: A finite geometric underpinning for form theories of gravity and black hole entropy. *Physical Review D*, 96(2), 026018.

- [27] Planat, M., Saniga, M., & Holweck, F. (2013). Distinguished three-qubit ‘magicity’ via automorphisms of the split Cayley hexagon. *Quantum information processing*, 12(7), 2535-2549.
- [28] Lévy, P., Planat, M., & Saniga, M. (2013). Grassmannian connection between three- and four-qubit observables, Mermin’s contextuality and black holes. *Journal of High Energy Physics*, 2013(9), 1-35.
- [29] de Boutray, H., Holweck, F., Giorgetti, A., & Masson, P. A. (2021). Automated synthesis of contextuality proofs from subspaces of symplectic polar spaces. arXiv preprint [arXiv:2105.13798](https://arxiv.org/abs/2105.13798).
- [30] Maldeghem, van H., *Generalized Polygons, Monographs in Mathematics 93*, Birkhäuser, Basel, 1998.
- [31] Schroth, A. E. (1999). How to draw a hexagon. *Discrete Math*, 199, 161-171.
- [32] Saniga, M., Planat, M., Pracna, P., & Lévy, P. (2012). ‘Magic’ Configurations of Three-Qubit Observables and Geometric Hyperplanes of the Smallest split Cayley hexagon. *SIGMA. Symmetry, Integrability and Geometry: Methods and Applications*, 8, 083.
- [33] Polster, B., Schroth, A. E., & Van Maldeghem, H. (2001). Generalized flatland. *The Mathematical Intelligencer*, 23(4), 33-47.